

# Preparation and sensing characterization of hybrid iron oxide/polyaniline/reduced graphene oxide at room temperature

<sup>1</sup>Nurul Athirah Abu Hussein, <sup>1</sup>Huzein Fahmi Hawari\*, <sup>2</sup>Wong Yew Hoong and <sup>2</sup>A.S.M.A Haseeb

<sup>1</sup>Department of Electrical and Electronic, Universiti Teknologi PETRONAS, 32610, Seri Iskandar, Perak, Malaysia and

<sup>2</sup>Centre of Advanced Materials, Department of Mechanical Engineering, Faculty of Engineering, University Malaya 50603 Kuala Lumpur, Malaysia

## Abstract

Building materials, plants, paints, chemicals, and fossil fuels combustions all emanate volatile organic compound (VOC), which influence our health and everyday lives. Therefore, the ability to detect VOCs at room temperature is very essential. This study focused on interdigitated electrode (IDE) sensor based on the hybrid nanoparticles of iron oxide (Fe<sub>3</sub>O<sub>4</sub>), polyaniline (PANI) and reduced graphene oxide (rGO) and its sensing mechanism towards 300ppm acetone was investigated. The hybrid material was synthesized through in-situ method and deposited on the IDE using drop-cast method. X-ray diffraction shows that all unary materials were present in the hybrid nanoparticles and the crystallite size calculated was 4.49nm. The response and recovery time for the hybrid material towards 300ppm acetone was 2.73min and 2.67min, respectively which shows a great improvement compared to response and recovery time of single material of Fe<sub>3</sub>O<sub>4</sub>. The IDE based on hybrid materials sensor is sensitive and reversible, making it suitable for human health and environmental safety application.

**Keywords:** Interdigitated electrode (IDE), hybrid material, volatile organic compound (VOC), sensing application

Full length article \*Corresponding Author, e-mail [huzeinfahmi.hawari@utp.edu.my](mailto:huzeinfahmi.hawari@utp.edu.my)

## 1. Introduction

One of the major sources of environmental problems in recent years has been the emission of hazardous compounds from various factories. To ensure a safe living environment, trace sensing devices are required to detect these gases [1, 2]. Sensors for detecting these gases at trace levels are critical for maintaining a safe living environment. In this way, many forms of gas sensors were used for detecting these gases such as calorimetric [3], conductometric [4], potentiometric [5], catalytic [6] and chemical [7]. The chemiresistive sensors were widely used because of their high selectivity, sensitivity, ease of processing, compact in size, lower process temperature and low electrical consumption. Due to some drawbacks of the sensors mentioned above, nowadays, the advances in low temperature processing nanomaterials have enabled alternate ways for embedding sensor layers on diverse substrates in a straightforward manner like IDE [8].

IDE is one of the most promising approaches to dealing with the problems of sensitivity, simple, user-friendly, reliable, fast, less expensive, portable and multi-analyte detection. Sensors of various types have been developed for food, water, security, agriculture, military, and medical quality control which has been a promising platform as it provides miniaturization of electrodes in sensor devices [9-12]. Despite of the design of the sensor platform, the selection of materials as the active layer of the sensor also plays a crucial part to improve the performance of the sensor.

Metal oxide-based gas sensors are the most promising for monitoring hazardous volatile organic compounds (VOC). They are in high demand in a variety of fields, owing to their numerous advantages, which include strong response, small dimensions, ease of use, fast response, stable repeatability for reuse in the same process, simplicity in fabrication, low detection limits, inexpensive and low energy consumption [13-15]. Among the huge variety of materials studied, inorganic semiconductor oxides (usually SnO<sub>2</sub>, ZnO, TiO<sub>2</sub> and Fe<sub>2</sub>O<sub>3</sub>) have garnered the

greatest attention and constitute a significant portion of commercially available gas sensors [16-18]. In recent years, there have been further advancement in the comprehension of metal oxide that can be exploited for gas sensing application and new material hybridization have been recognized that may improve the sensor performance such as lowering the operating temperature of metal oxide semiconductor (MOX) sensor [19, 20].

Carbon nanotubes and graphene stand out among the carbon-based materials due to their high carrier mobility (conductive qualities), high quality crystal lattices, and low electrical noise. Furthermore, their excellent mechanical and thermal qualities make them ideal for flexible electrical devices. While having great conducting properties, carbon nanostructures have a number of drawbacks for sensor applications, including a long recovery time, insufficient selectivity, and poor interaction with gas molecules. Carbon nanomaterials can therefore be synthesized by functionalizing or combining them with other materials to create hybrid platforms with improved sensing capability, for the detection of VOC [21].

As a result, in this study, we will functionalize graphene with metal oxide nanomaterial to open a large energy gap in graphene via the quantum confinement effect in order to increase sensor performance.

## 2. Materials and methods

### 2.1. Materials

Iron (II) chloride tetrahydrate ( $\text{FeCl}_2 \cdot 4\text{H}_2\text{O}$ ), iron (III) chloride hexahydrate ( $\text{FeCl}_3 \cdot 6\text{H}_2\text{O}$ ), iron (III) nitrate ( $\text{Fe}(\text{NO}_3)_3 \cdot 9\text{H}_2\text{O}$ , nitric acid (65%), hydrochloric acid (37%), ascorbic acid and graphene oxide (GO) paste (95 wt% purity) was all purchased from Merck. De-ionized (DI) water is used in all preparations. IDE with size of 5mm  $\times$  5mm was purchased from NovaScientific.

### 2.2. Synthesis of iron oxide ( $\text{Fe}_3\text{O}_4$ )

$\text{Fe}_3\text{O}_4$  was synthesized using Massart's procedure as mentioned in [22, 23] by mixing  $\text{FeCl}_3$  and  $\text{FeCl}_2$  together. The mixture was added to ammonium hydroxide solution. The instantaneous black magnetite precipitate ( $\text{Fe}_3\text{O}_4$ ) was formed. The solution was washed with DI water a few times and nitric acid was added to it. Finally, ferric nitrate solution was mixed in the solution to obtain the final product. The procedure is illustrated in Figure 1.

### 2.3. Synthesis of polyaniline (PANI)

The conducting polymer, PANI was prepared by chemical oxidative polymerization of aniline. In the presence of hydrochloric acid HCl and ammonium peroxydisulphate (APS) were used as oxidants. First, 1 M of Hussein et al., 2021

HCl protonic acid and 0.2M of aniline monomer solution were placed in a beaker and mixed at a temperature of about  $-4^\circ\text{C}$ . Then 0.25M of APS was added into the above solution in an aqueous medium using the dropped wise method. Both solutions were mixed in a beaker and stir to polymerize the mixture. The precipitate PANI was collected, filtrate and washed as mentioned in the previous work [22].

### 2.4. Synthesis of rGO

The rGO was prepared according to previous work [24, 25, 26] where 10g of ascorbic acid with 100ml of distilled water and stirred in 0.1mg/ml of GO solution. The, the sample was heated up at  $95^\circ\text{C}$  for 1 hour and sonicated for about 15mins, filtered, and washed with distilled water.

### 2.5. Synthesis of the hybrid material

The hybrid material was prepared using in-situ method where 10wt% of iron oxide and PANI were dissolved in GO paste with ascorbic acid solution and heated up for 1 hour at  $95^\circ\text{C}$  before being centrifuged and washed for few times.

## 3. Results and discussion

### 3.1. Microstructural study analysis (XRD)

Figure 2 shows the typical XRD pattern of  $\text{Fe}_3\text{O}_4$  nanoparticles (NPs) synthesized using Massart's procedure. It is clear that the cubic spinel structure of  $\text{Fe}_3\text{O}_4$  NPs occurred at the angles of  $2\theta = 30.4^\circ, 35.6^\circ, 43.1^\circ, 57.2^\circ$  and  $62.7^\circ$  with planes of (200), (311), (400), (511) and (440), respectively. All diffraction peaks are indexed to cubic spinel structure of  $\text{Fe}_3\text{O}_4$  NPs with lattice constant,  $a = 8.39 \text{ \AA}$ . The results are consistent with pure  $\text{Fe}_3\text{O}_4$  NPs phase (ICDD No. 96-151-3305). The diffraction pattern of PANI can be observed at a range of  $2\theta: 9.21^\circ, 14.96^\circ, 20.79^\circ, 25.43^\circ, 27.01^\circ$  and  $29.89^\circ$  which corresponding to  $d_{9.6}, d_{5.9}, d_{4.2}, d_{3.5}, d_{3.3}$  and  $d_{2.9}$ . Based on the XRD pattern of rGO, a small peak can be seen approximately at  $16.3^\circ$ . According to Jayachandiran et al. (2018), when reducing rGO from Graphene Oxide (GO), the diffraction peak at around  $11^\circ$  will disappeared and will be replaced by a new peak at around  $24^\circ$  which correlate to the removal of oxygen functional groups during the reduction process of GO [27].

However, in Figure 3, a broad peak was present approximately at  $4-14^\circ$  and  $25-40^\circ$ . This might be due to incomplete process of reduction from GO to rGO. The incomplete process is because of the concentration of GO in the solution [28]. The peak of the hybrid material occurred at the angles of  $2\theta=25.36^\circ, 30.45^\circ, 35.72^\circ, 43.47^\circ, 57.43^\circ$  and  $63.02^\circ$ . These peaks are in accordance with all the single materials where the peaks along  $2\theta: 14-30^\circ$  is related to the interaction of PANI and graphene and the rest of the peaks are in accordance with  $\text{Fe}_3\text{O}_4$ . The crystallite size of

these materials was calculated using Debye-Scherrer Equation,

$$D = \frac{K\lambda}{\beta \cos\theta}$$

Where D is the average crystallite size in nm, k is the shape factor, often assigned a value of 0.9, λ is the x-ray wavelength of x-ray radiation (1.54Å), β is the full width at half maximum (FWHM) measured in radians, θ is the half angle measured in degrees. The crystallite size of Fe<sub>3</sub>O<sub>4</sub>, PANI and hybrid sample was calculated to be 6.34, 5.5 and 4.49nm respectively.

**3.2. Sensing characterization**

The sensor responses of the single material Fe<sub>3</sub>O<sub>4</sub> and the hybrid that contains 10wt% of Fe<sub>3</sub>O<sub>4</sub> and PANI were shown in Figure 4 and 5 upon exposure to 300ppm of acetone. The single material Fe<sub>3</sub>O<sub>4</sub> was conducted at 300°C while the hybrid sample was conducted at room

temperature. All samples were first purged with nitrogen for about 5min and purged with acetone. The sensor’s response as a change in resistance and the response as well as the recovery time were studied. The change in the response of the sensor is due to the change in the texture and size of the active material [8]. The base resistance of the single material is higher compared to the hybrid sample. The response of the hybrid sample was decreased to 2.6%.

This is because smaller sample have higher surface area which can absorb more analyte and eventually increase the sensitivity of the sensor. The response and recovery time for both Fe<sub>3</sub>O<sub>4</sub> and hybrid samples were 2.19/3.6min and 2.73/2.67min, respectively. This shows an increasing of response time and decreasing of recovery time after the sample is being hybridized, however the operational temperature of the sensor has been reduced to room temperature. It is clear that IDE sensor based on the hybrid materials has better sensitivity when compared to single material Fe<sub>3</sub>O<sub>4</sub>.

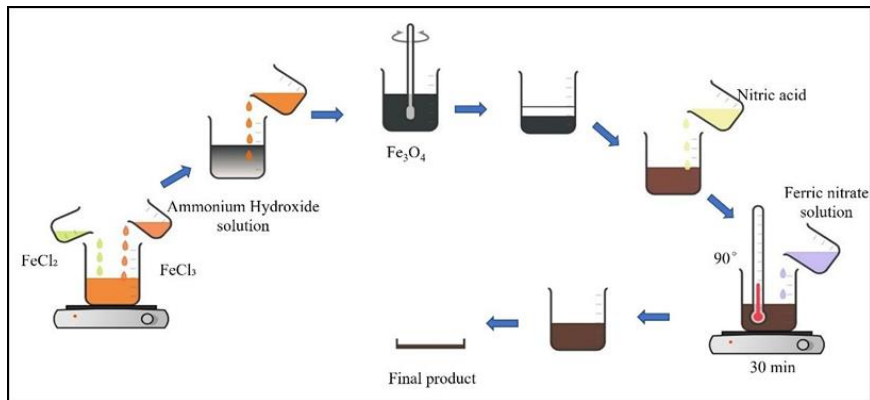


**Fig. 1:** Synthesis procedure of Fe<sub>3</sub>O<sub>4</sub>

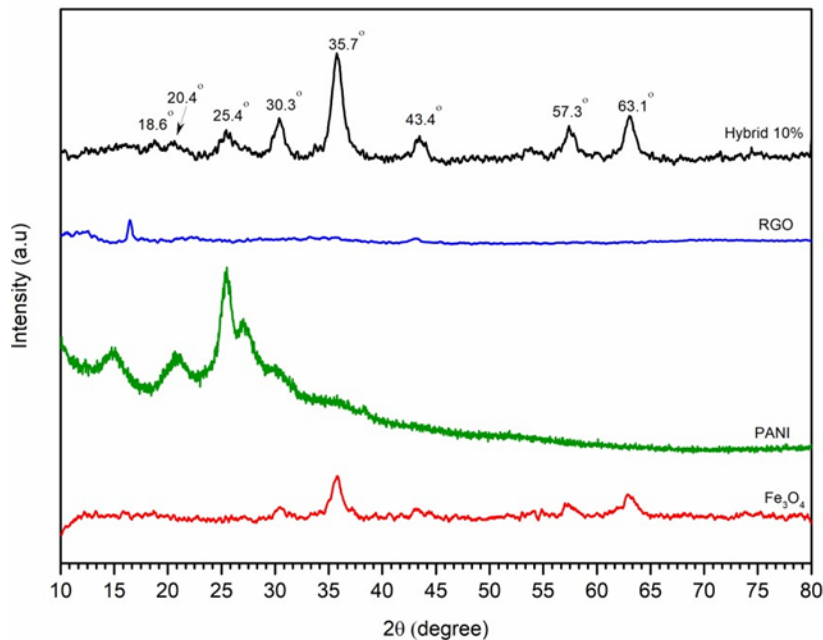


**Fig. 2:** XRD pattern for all samples

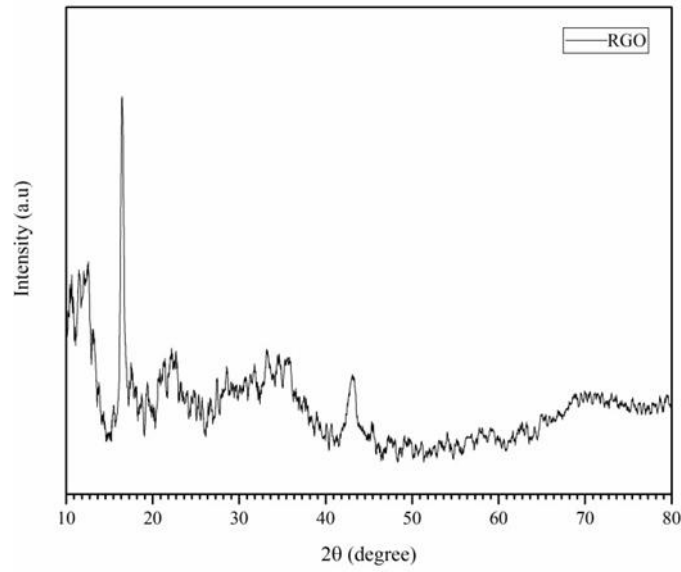


**Fig. 3:** XRD pattern for rGO

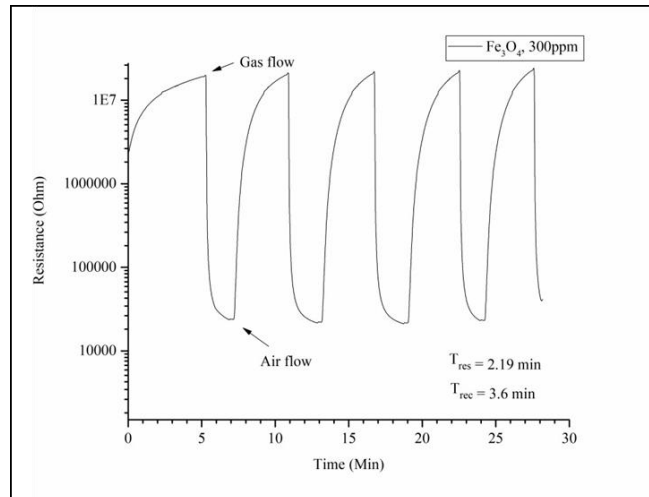


**Fig. 4:** Sensor response for single material  $\text{Fe}_3\text{O}_4$  at  $300^\circ\text{C}$

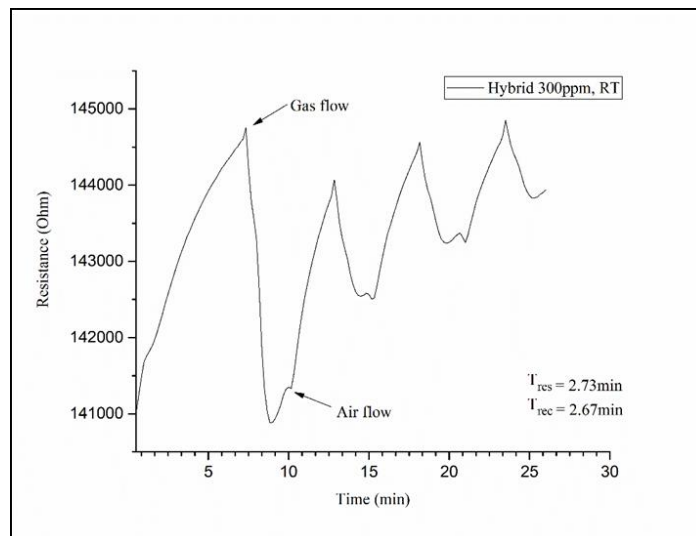


**Fig. 5:** Sensor response for hybrid nanomaterial at room temperature

#### 4. Conclusions

In general, the fabrication of ternary hybrid nanocomposite materials has been synthesized and the characterization analysis shows that the ternary hybrid material exhibits a great composition where they can blend homogeneously together. XRD analysis showed that all peaks from the hybrid nanocomposite matched well with the individual materials and the crystallite size calculated are less than 10nm. From the sensing characteristic, the response and recovery time of unary material Fe<sub>3</sub>O<sub>4</sub> was 2.19min and 3.6 min, respectively at operational temperature of 300°C. However, when it was hybridized with PANI and rGO, the operational temperature can be lowered down to room temperature and response and recovery time was 2.73min and 2.67min, respectively. This shows that the hybrid material can create a great synergistic effect as active sensing material to improve the sensing performance of the IDE. However, further studies need to be done to investigate the chemical and physical characteristic of the active materials so that alteration can be made to further lower down the response and recovery time as well as improve the sensitivity of the sensor.

#### Acknowledgements

This work was financially supported by Ministry of Higher Education through the Fundamental Research Grant Scheme FRGS (FRGS Code: (FRGS/1/2019/TK04/UTP/02/7).

#### References

- [1] D. Zhang, C. Jiang, Y. Yao, D. Wang and Y. Zhang. (2017). Room-temperature highly sensitive CO gas sensor based on Ag-loaded zinc oxide/molybdenum disulfide ternary nanocomposite and its sensing properties. *Sensors and Actuators B: Chemical*. 253: 1120-1128.
- [2] P. Srinivasan, M. Ezhilan, A.J. Kulandaisamy, K.J. Babu and J.B.B. Rayappan. (2019). Room temperature chemiresistive gas sensors: Challenges and strategies—A mini review. *Journal of Materials Science: Materials in Electronics*. 30 (17) 15825-15847.
- [3] V. Kitsos, A. Demosthenous and X. Liu. (2019). A smart dual-mode calorimetric flow sensor. *IEEE Sensors Journal*. 20 (3) 1499-1508.
- [4] U. Latif, L. Ping and F.L. Dickert. (2018). Conductometric sensor for PAH detection with molecularly imprinted polymer as recognition layer. *Sensors*. 18 (3) 767.
- [5] X. Liu, Y. Yao, Y. Shao, J. Wu, Y. Ying and J. Ping. (2020). Phase-dependent ion-to-electron transducing efficiency of WS<sub>2</sub> nanosheets for an all-solid-state potentiometric calcium sensor. *Microchimica Acta*. 187 (9) 1-9.
- [6] Y.K. Moon, S.Y. Jeong, Y.C. Kang and J.H. Lee. (2019). Metal oxide gas sensors with Au nano-cluster catalytic over layer: toward tuning gas selectivity and response using a novel bilayer sensor design. *ACS Applied Materials and Interfaces*. 11 (35) 32169-32177.
- [7] P. Kumar, K.H. Kim, P.K. Mehta, L. Ge and G. Lisak. (2019). Progress and challenges in electrochemical sensing of volatile organic compounds using metal-organic frameworks. *Critical Reviews in Environmental Science and Technology*. 49 (21) 2016-2048.
- [8] S. Khan, S. Ali and A. Bermak. (2019). Substrate dependent analysis of printed sensors for detection of volatile organic compounds. *IEEE Access*. 7: 134047-134054.
- [9] R.D.A.A Rajapaksha, U. Hashim, S.C.B. Gopinath and C.A.N. Fernando. (2018). Sensitive pH detection on gold inter-digitated electrodes as an electrochemical sensor. *Microsystem Technologies*. 24 (4) 1965-1974.
- [10] F. Alexander Jr., D.T. Price and S. Bhansali. (2010). Optimization of interdigitated electrode (IDE) arrays for impedance based evaluation of Hs 578T cancer cells. In *Journal of Physics: Conference Series*. 224 (1) 012134.
- [11] R. Daly, T. Narayan, H. Shao, A. O’Riordan and P. Lovera. (2021). Platinum-Based Interdigitated Micro-Electrode Arrays for Reagent-Free Detection of Copper. *Sensors*. 21 (10) 3544.
- [12] O. Fysun, A. Schmitt, P.T. Auernhammer, J. Rauschnabel and H.C. Langowski. (2019). Electrochemical detection of food-spoiling bacteria using interdigitated platinum microelectrodes. *Journal of Microbiological Methods*. 161: 63-70.
- [13] A. Mirzaei, S.G. Leonardi and G. Neri. (2016). Detection of hazardous volatile organic compounds (VOCs) by metal oxide nanostructures-based gas sensors: A review. *Ceramics International*. 42 (14) 15119-15141.
- [14] I. Simon, N. Bârsan, M. Bauer and U. Weimar. (2001). Micromachined metal oxide gas sensors: opportunities to improve sensor performance. *Sensors and Actuators B: Chemical*. 73 (1) 1-26.
- [15] D. Zappa, V. Galstyan, N. Kaur, H.M.M. Arachchige, O. Sisman and E. Comini. (2018). “Metal oxide-based heterostructures for gas sensors”—A review. *Analytica Chimica Acta*. 1039: 1-23.

- [16] S. Liang, J. Li, F. Wang, J. Qin, X. Lai and X. Jiang. (2017). Highly sensitive acetone gas sensor based on ultrafine  $\alpha$ -Fe<sub>2</sub>O<sub>3</sub> nanoparticles. *Sensors and Actuators B: Chemical*. 238: 923-927.
- [17] F.A. Harraz, M. Faisal, A.A. Ismail, S.A. Al-Sayari, A.E. Al-Salami, A. Al-Hajry and M.S. Al-Assiri. (2019). TiO<sub>2</sub>/reduced graphene oxide nanocomposite as efficient ascorbic acid amperometric sensor. *Journal of Electroanalytical Chemistry*. 832: 225-232.
- [18] P.G. Su and L.Y. Yang. (2016). NH<sub>3</sub> gas sensor based on Pd/SnO<sub>2</sub>/RGO ternary composite operated at room-temperature. *Sensors and Actuators B: Chemical*. 223: 202-208.
- [19] C. Zhang, Y. Luo, J. Xu and M. Debliqy. (2019). Room temperature conductive type metal oxide semiconductor gas sensors for NO<sub>2</sub> detection. *Sensors and Actuators A: Physical*. 289: 118-133.
- [20] Z. Li, H. Li, Z. Wu, M. Wang, J. Luo, H. Torun and Y. Fu. (2019). Advances in designs and mechanisms of semiconducting metal oxide nanostructures for high-precision gas sensors operated at room temperature. *Materials Horizons*. 6 (3) 470-506.
- [21] R.S. Andre, R.C. Sanfelice, A. Pavinatto, L.H. Mattoso and D.S. Correa. (2018). Hybrid nanomaterials designed for volatile organic compounds sensors: A review. *Materials and Design*. 156: 154-166.
- [22] N.A.A. Hussein, H.F. Hawari and Y.H. Wong. (2021). Synthesis of Iron Oxide / Polyaniline / Reduced Graphene Oxide Nanocomposite Materials as Active Sensing Material. "2020 8<sup>th</sup> International Conference on Intelligent and Advanced Systems (ICIAS)", Kuching, Malaysia. July 13-15 2021.
- [23] A.H. Nurul Athirah, B.C. Ang, Y.H. Wong, B.H. Ong, A.A. Baharuddin. (2018). "Synthesis and characterization of  $\gamma$ -Fe<sub>2</sub>O<sub>3</sub> NPs on silicon substrate for power device application." *Materials Research Express*. 5(6).
- [24] Z.Y. Lee, H.F.B. Hawari, G.W.B. Djaswadi, and K. Kamarudin. (2021). A highly sensitive room temperature CO<sub>2</sub> gas sensor based on SnO<sub>2</sub>-rGo hybrid composite. *Materials*. 14 (3) 522.
- [25] M. Gupta, H.F. Hawari, P. Kumar, Z.A. Burhanudin and N. Tansu. (2021). Functionalized Reduced Graphene oxide thin films for ultrahigh CO<sub>2</sub> gas sensing performance at room temperature. *Nanomaterials*. 11 (3) 623.
- [26] H.F. Hawari and A. Faisal Ahmad Zaki. "Development of rGO based Gas Sensor for Acetone Detection. "2021 IEEE International Conference on Sensors and Nanotechnology (SENNANO)", Port Dickson, Malaysia, September 22-24 2021.
- [27] J. Jayachandiran, J. Yesuraj, M. Arivanandhan, A. Raja, S.A. Suthanthiraraj, R. Jayavel and D.J.J.O.I. Nedumaran. (2018). Synthesis and electrochemical studies of rGO/ZnO nano-composite for super capacitor application. *Journal of Inorganic and Organometallic Polymers and Materials*. 28 (5) 2046-2055.
- [28] S.A. Soomro, I.H. Gul, H. Naseer, S. Marwat and M. Mujahid. (2019). Improved performance of CuFe<sub>2</sub>O<sub>4</sub>/rGO nanohybrid as an anode material for lithium-ion batteries prepared via facile one-step method. *Current Nanoscience*. 15 (4) 420-429.